

Influence of ZnO Co-Doping On the Structural, Optical, and Antibacterial Properties of $(\text{Zn}_{1-2x}\text{Ce}_x\text{Fe}_x)\text{O}$ Nanoparticles

J.Arul Mary¹, J. Judith Vijaya²Catalysis & Nanomaterials Research Laboratory, Department of Chemistry, Loyola College (Autonomous), Chennai, Tamil Nadu, India^{1,2}

ABSTRACT: Pure and co-doped ZnO nanoparticles were synthesized by microwave combustion method using urea as a fuel. Structural, optical, morphological and magnetic property was studied using X-ray diffraction (XRD), scanning electron microscopy (SEM), diffuse reflectance spectroscopy (DRS), and photoluminescence (PL) spectra. X-ray diffraction measurements of the nanoparticles showed the same wurtzite hexagonal structure and preferential orientation along the c-axis. The scanning electron microscope image of the nanoparticles revealed an average particle size of 47-23 nm. The calculated results from DRS spectroscopy indicated that the band gap of the synthesized samples decreased with the increment of the concentration of co-dopant, which resulted in the red-shift. The photoluminescence (PL) studies revealed that violet, blue and green emissions. The well diffusion method was used for antibacterial activities of two Gram negative and three Gram positive bacterial pathogens. The doping with Ce and Fe by microwave method improves the antibacterial property.

KEYWORDS: ZnO, Band gap, microwave combustion, semiconductors, ferromagnetism.

I. INTRODUCTION

Nanostructured materials offer promising opportunities for the enhanced and tailored properties for application in environmental catalysis, due to their unique physicochemical properties, caused by their nanosized dimensions and large surface/volume ratios [1]. Metal oxide nanostructures such as, TiO_2 , ZnO, CuO, SiO_2 , SnO_2 and MgO have shown great potential in biomedical sector, due to their tremendous properties at nano scale, such as, optical, catalytic and antibacterial properties. Among these metal oxides nanomaterials, ZnO is of special attention, due to its established use in healthcare products, UV blocking capability, biocompatibility and modest cost [2]. Microbial contamination is a serious issue in healthcare and food industry so that the development of antimicrobial agents and surface coatings has been attracting increasing attention in recent years [3]. Therefore, developments of nanostructures with antimicrobial properties are of extensive interest. Meanwhile, doping in ZnO alters the band-gap, optical, electrical, non-linear optical and magnetic properties. Among the dopants, transition and rare earth metals have gained much attention. The microwave combustion method is a potential method for the production of technologically useful materials, as it has the advantages of time saving, low external energy consumption, self sustaining instantaneous reaction, and high yield of nanosized particles [4]. In the present study, we report the synthesis and characterization of undoped and Ce, Fe co-doped ZnO nanoparticles, and their antibacterial studies.

II. EXPERIMENTAL PART

ZnO powders were prepared with the addition of Fe and Ce of different molar ratios ($(\text{Zn}_{1-2x}\text{Fe}_x\text{Co}_x)\text{O}$ with $x = 0.00, 0.01, 0.02, 0.03, 0.04$ and 0.05) to ZnO. The precursors mixture in urea is dissolved in de-ionized water by using magnetic stirrer for 30 min, then poured into a crucible. After that, the crucible is placed into a microwave oven operating at 800 W for 8 min till the precursors solution mixture decomposes. When the solution reaches the point of

spontaneous combustion, it begins to release heat by burning and turns into a solid powder. After the completion of the reaction, the obtained solid powder is washed, and then annealed at 600°C for 2 h.

III. CHARACTERIZATIONS

Structural characterization of pure and Ce, Fe co-doped ZnO was performed using a Rigaku Ultima IV high resolution X-ray diffractometer (XRD) with CuK α radiation ($\lambda = 1.5418 \text{ \AA}$). Morphological studies and energy dispersive X-ray analysis have been performed with a Jeol JSM6360 high resolution scanning electron microscope (HR-SEM). UV-Visible diffuse reflectance spectrum (DRS) was recorded using Cary100 UV-Visible spectrophotometer to estimate the energy band gap. The photoluminescence (PL) properties were recorded by using Varian Cary Eclipse fluorescence spectrophotometer. The antibacterial activity of Gram-negative, and Gram-positive pathogens was determined by well diffusion method. About 25 mL of molten Mueller Hinton Agar was poured into a sterile Petri plate. Plates were allowed to solidify, after which 18 h grown (OD adjusted 0.6) 100 μl of above said pathogenic bacteria cultures were transferred onto the plate and made culture lawn by using sterile L-rod spreader. After 5 min setting of the bacteria, the wells were made using sterile 5 mm cork borer and the test samples were dissolved in sterile water at various concentrations (i.e. 25, 50, 75 and 100 $\mu\text{l}/\text{well}$). The sterile water served as control. The plates were incubated at 37°C in a 40 W fluorescent light source ($\sim 400 \text{ nm}$) for 24 h. The antibacterial activity was determined by measuring the diameter of the zone of inhibition around the well using antibiotic zone scale in millimeter (mm).

IV. RESULTS AND DISCUSSION

1. XRD ANALYSIS

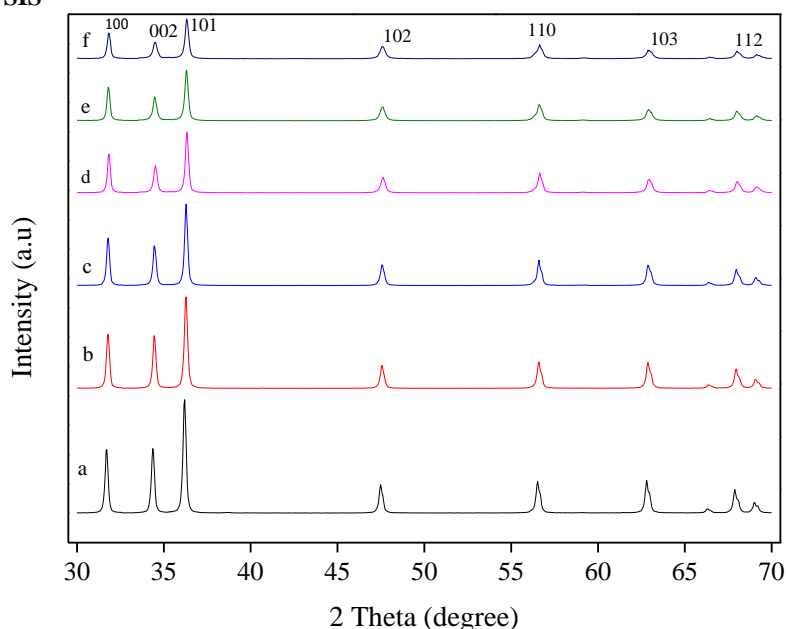


Figure 1. (a–f) XRD patterns of (a) pure ZnO, (b) $\text{Zn}_{0.98}\text{Ce}_{0.01}\text{Fe}_{0.01}\text{O}$, (c) $\text{Zn}_{0.96}\text{Ce}_{0.02}\text{Fe}_{0.02}\text{O}$, (d) $\text{Zn}_{0.94}\text{Ce}_{0.03}\text{Fe}_{0.03}\text{O}$, (e) $\text{Zn}_{0.92}\text{Ce}_{0.04}\text{Fe}_{0.04}\text{O}$, (f) $\text{Zn}_{0.90}\text{Ce}_{0.05}\text{Fe}_{0.05}\text{O}$ samples

X-ray diffraction (XRD) patterns of all samples in Fig. 1, display sharp and intensive peaks of typical hexagonal wurtzite structure of ZnO (JCPDS no. 89-0510). The peaks slightly shifted towards larger diffracted angles, peak intensity gradually decreases and is attributed to the difference in the ionic radii of Ce^{3+} and Fe^{2+} ions as compared to that of Zn^{2+} ($\text{Zn}^{2+} = 0.074 \text{ nm}$, $\text{Ce}^{3+} = 0.103 \text{ nm}$ and $\text{Fe}^{2+} = 0.077 \text{ nm}$). The crystallite size of the prepared nanoparticles is estimated by using Scherrer's formula,

$$L = \frac{0.89 \lambda}{\beta \cos \theta} \quad (1)$$

where, L is the crystallite size, λ , the X-ray wavelength, θ , the Bragg diffraction angle and β , the full width at half maximum (FWHM) [5]. The calculated results shown in Table. 1 revealed that the average size of the crystals increased with an increase in the concentration of the dopants.

Table 1. Lattice parameter, crystallite size (Scherrer formula) and band gap values of $(Zn_{1-2x}Ce_xFe_x)O$ ($x = 0.00, 0.01, 0.02, 0.03, 0.04$ and 0.05) system

Samples	Crystallite size (nm) Scherrer formula	Band gap (eV)	Lattice parameter
Pure ZnO	35.36	3.22	a =3.2491 c=5.2035
$Zn_{0.98}Ce_{0.01}Fe_{0.01}O$	35.39	3.16	a=3.2499 c=5.2041
$Zn_{0.96}Ce_{0.02}Fe_{0.02}O$	36.76	3.10	a=3.2508 c=5.2045
$Zn_{0.94}Ce_{0.03}Fe_{0.03}O$	37.42	3.08	a=3.2513 c=5.2061
$Zn_{0.92}Ce_{0.04}Fe_{0.04}O$	37.74	3.05	a=3.2517 c= 5.2061
$Zn_{0.90}Ce_{0.05}Fe_{0.05}O$	37.92	3.01	a=3.2536 c=5.2110

2. SCANNING ELECTRON MICROSCOPY (SEM) STUDIES.

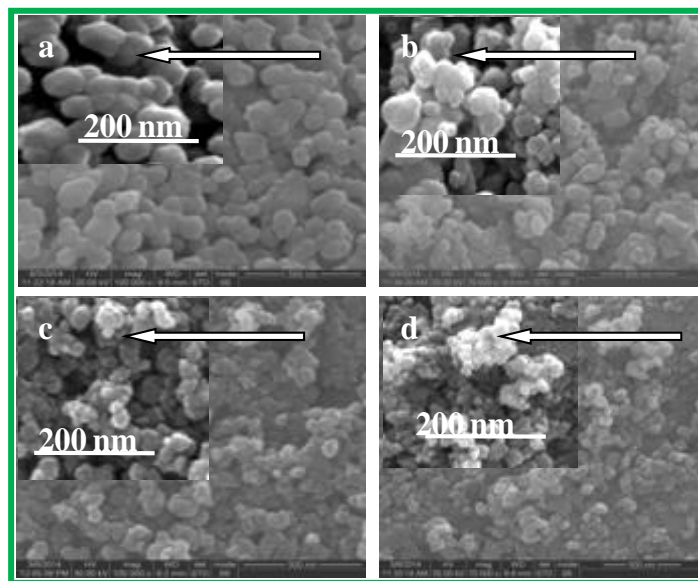


Figure 2. (a–d) HR-SEM images of (a) pure ZnO, (b) $Zn_{0.98}Ce_{0.01}Fe_{0.01}O$, (c) $Zn_{0.94}Ce_{0.03}Fe_{0.03}O$, (d) $Zn_{0.90}Ce_{0.05}Fe_{0.05}O$ samples.

The HRSEM micrographs of the nanostructures synthesized by microwave combustion method are shown in Fig. 2. Fig. 2(a) exhibits the hexagonal platforms like morphology for undoped ZnO. A magnificent change in shape of ZnO nanostructures was observed in co doped ZnO. When the co dopant concentrations were increased from 0.01 to 0.05 M, the grains shape are converted to spherical shape with the same wurtzite structure. However, further increase in co dopant concentration led to dwindling in the spherical structure. The particle size of the Ce Fe co-doped ZnO samples decreased with an increase in the concentration of iron and cerium. Upon further increase in the Ce³⁺ and Fe²⁺ content, the particle size decreased from 37 to 27nm, which is much smaller than pure ZnO.

3. OPTICAL PROPERTIES (Diffuse Reflectance Spectroscopy)

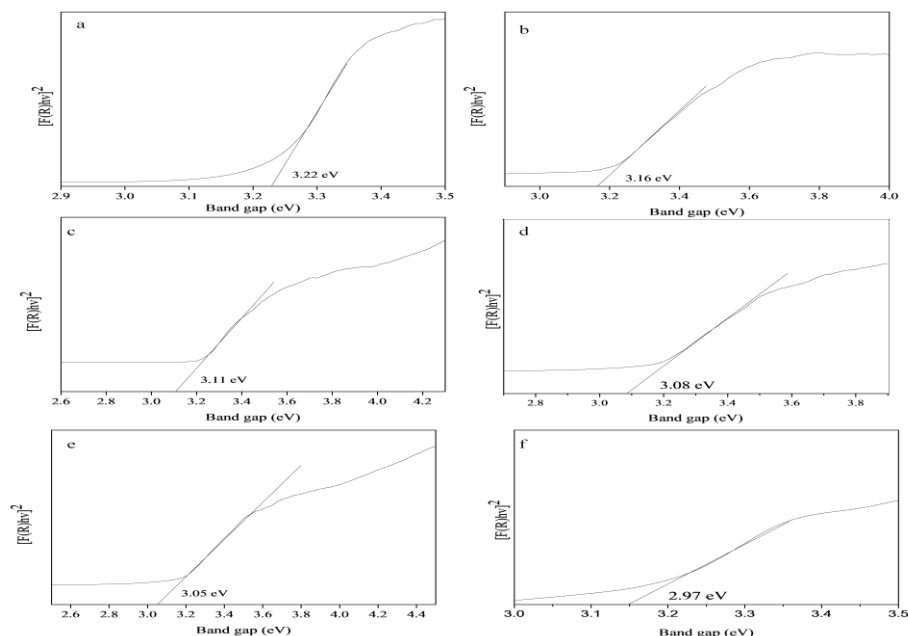


Figure 3. (a-f) UV–Visible diffuse reflectance spectra of $(Zn_{1-2x}Ce_xFe_x)O$ ($x = 0.00, 0.01, 0.02, 0.03, 0.04$ and 0.05) system

The diffuse reflectance spectra of Ce, Fe co-doped ZnO samples in the range of 200-800 nm at room temperature were examined to determine their optical absorption properties. The reflectance spectra were analyzed using a modified Kubelka-Munk function $F(R)$ [6] estimated from the following equation,

$$F(R) = (1-R)^2/2R \quad (2)$$

$F(R)$ is the Kubelka– Munk function, where R is the reflectance. A graph was plotted between $[F(R)hv]^2$ and hv , and the intercept value obtained corresponds to the band gap energy. It is evident that the band gaps decreased with the increase in co-dopant concentration. This red shift of the band gap edge is due to the incorporation of Ce and Fe elements into ZnO lattice.

4. PHOTOLUMINESCENCE ANALYSIS (PL)

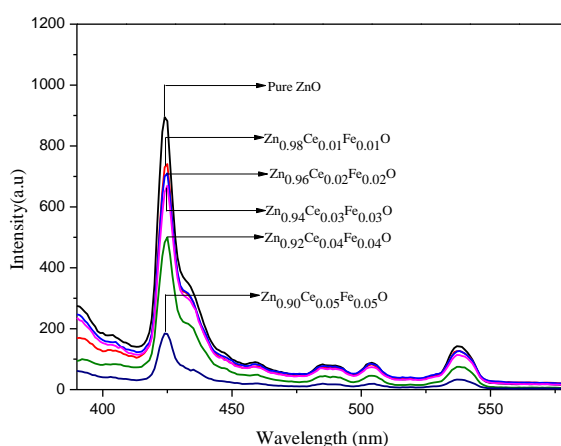


Figure 4. PL spectra of $Zn_{1-2x}Ce_xFe_xO$ ($x = 0.00, 0.01, 0.02, 0.03, 0.04$ and 0.05) system.

Fig. 4 exhibits the photoluminescence spectra of undoped and co-doped ZnO samples taken at room temperature employing the excitation wavelength of 325 nm. The visible or deep trap state emissions (424, 458, 483, 490, 504 and 537 nm) are generally defined as the recombination of the electron hole pair from the localized states with the energy levels deep seated in the band gap, producing lower energy emissions. The green light emission centered at 490 nm can be traced to an oxygen vacancy (VO) [7]. The blue emission at 458 and 483 nm is associated to the defect structure of the material. Hence, the blue emission peak was ascribed to the electron transition from both the interstitial Zn levels to the valence band and the energy levels of interstitial Zn to Zn vacancies. A broad PL band in the green region at 537 nm is attributed to the defect levels associated with oxygen vacancies or zinc interstitial [8].

5. ANTIBACTERIAL ACTIVITY

Table 2: Antibacterial activity of the samples against pathogens

Sample code	Antibacterial activity of the sample zone of inhibition (mm)																			
	<i>Staphylococcus aureus</i>				<i>Klebsiellapneumoniae</i>				<i>Escherichia coli</i>				<i>Pseudomonas aeruginosa</i>				<i>Bacillus subtilis</i>			
Conc. (μ l/well)	25	50	75	100	25	50	75	100	25	50	75	100	25	50	75	100	25	50	75	100
ZnO	--	3	7	9	--	5	7	8	--	7	9	12	--	5	9	12	--	6	9	11
$Zn_{0.94}Ce_{0.03}Fe_{0.03}O$	5	7	11	15	6	10	13	16	6	10	12	17	6	9	12	15	7	9	11	14
$Zn_{0.90}Ce_{0.05}Fe_{0.05}O$	14	20	21	24	19	20	22	25	15	18	21	24	16	21	26	28	12	13	21	23

International Journal of Innovative Research in Science, Engineering and Technology*An ISO 3297: 2007 Certified Organization**Volume 4, Special Issue 1, February 2015***THIRD NATIONAL CONFERENCE ON ADVANCES IN CHEMISTRY (NCAC – 2015)****On 18th February 2015****Organized by****Department of Chemistry, Easwari Engineering College (SRM Group of Institutions), Chennai-600089, India.**

In our study the relative antibacterial activity of undoped and co-doped ZnO nanoparticles towards Gram-negative *Pseudomonas aeruginosa*, *Escherichia coli* and Gram-positive *Staphylococcus aureus*, *Klebsiella pneumonia* and *Bacillus subtilis* bacterial pathogens are tested by well diffusion method. Table 2 shows the observed mean diameters inhibition zones for undoped and co-doped ZnO, which has increased from 26 and 28 mm against the given bacteria. From these zone measurements, it could be stated that co-doped ZnO possesses effective antibacterial property, when compared to ZnO nanoparticles. The antibacterial activity of nanoparticles can may either directly interact with the microbial cells (e.g. interrupting trans membrane electron transfer, disrupting/penetrating the cell envelope and oxidizing cell components) or produce secondary products (e.g. reactive oxygen species (ROS)) that cause damage.

V. CONCLUSION

A simple micro wave method has been employed to synthesize pure and co-doped ZnO nano structures. The structure, morphology, and antibacterial property have been investigated. Structure analyses indicate that the co dopants are incorporated into the ZnO host. Co doping enhances the optical and antibacterial property of the ZnO. The PL results showed that the optical properties of ZnO nanoparticles were enhanced by doping.

REFERENCES

1. N.L. Stock, J. S  ller, K. Vinodgal, P.V. Kamat, "Combinative sonolysis and photocatalysis for textile dye degradation", *Environ.Sci. Technol.* vol. 34, pp.1747–1750, 2000.
2. J. Sawai, T. Yoshikawa, "Quantitative evaluation of antifungal activity of metallic oxide powders (MgO, CaO and ZnO) by an indirect conductimetric assay", *J. Appl. Microbiol.* Vol. 96, pp. 803–809, 2004.
3. K.H. Tam, A.B. Djuricic, C.M.N. Chan, Y.Y. Xi, C.W. Tse, Y.H. Leung, W.K. Chan, "Antibacterial activity of ZnO nanorods prepared by a hydrothermal method", *Thin Solid Films* vol. 516, pp. 6167-6174, 2008.
4. K.C. Patil, S.T. Aruna, T. Mimani, "Combustion synthesis: an update", *Solid State Mater.* 6, 507-512, 2002.
5. E.S. Tuzemen, S. Eker, H. Kavak, R. Esen, "Dependence of film thickness on the structural and optical properties of ZnO thin films", *Appl. Surf. Sci.* vol. 255, pp. 6195-6200, 2007.
6. J. Hays, K.M. Reddy, N.Y. Graces, M.H. Engelhard, V. Shutthanandan, M. Luo, C. Xu, N.C. Giles, C. Wang, S. Thevuthasan, A. Punnoose, "Effect of Co doping on the structural, optical and magnetic properties of ZnO nanoparticles", *J. phys.Condens. Matter.* vol.19, pp.266203, 2007.
7. Z. Yan, Y. Ma, D. Wang, J. Wang, Z. Gao, L. Wang, P. Yu, T. Song, "Impact of annealing on morphology and ferromagnetism of ZnO nanorods" *Applied Phys. Lett.* Vol. 92, pp. 081911 – 081914, 2008.
8. J Ding, X.Yana, Q. Xue, "Study on field emission and photoluminescence properties of ZnO/graphene hybrids grown on Si substrates", *Mater. Chem. Phys.* Vol.133, pp.405–409, 2012.